

# Effect of MMF Harmonics on Single-Phase Induction Motor Performance – A Unified Approach

Mircea Popescu<sup>1</sup> Claus B Rasmussen<sup>2</sup> TJE Miller<sup>1</sup> Malcolm McGilp<sup>1</sup> and Calum Cossar<sup>1</sup>

1 – SPEED Laboratory, University of Glasgow, U.K.

2 – Grundfos A/S, 8550 Bjerringbro, Denmark

**Abstract**—Single-phase and two-phase induction machines are widely used in commercial applications due to their low cost and high reliability. The developed methods for the analysis of the single-phase induction motor, i.e. forward-backward field, symmetrical components and cross-field methods, can be adapted for modeling the MMF harmonics effect. This paper presents a unified approach on all these methods that demonstrates the equivalence between models and shows how the equivalent circuit elements can be interchanged from one method to another. Since half-cycle symmetry is a very common condition in the mass produced single-phase induction motors, this paper analyses only the odd MMF harmonic effects. Experimental results for three capacitor-run motors are used to validate all the proposed models.

**Index terms**—single-phase induction motors, MMF harmonics, electromagnetic torque

## I. LIST OF SYMBOLS

$V_m, V_a$  – complex voltages across main and auxiliary windings  
 $V_{p,n}, Z_{p,n}$  – complex positive/negative sequence voltage and impedance  
 $R_s, R_a, R_m$  – stator winding resistance: equivalent/auxiliary/main  
 $X_{ls}, X_{la}, X_{lm}$  – stator leakage reactance: equivalent/auxiliary/main  
 $a, a_n$  – effective turns ratio (aux / main)  
 $R_{rn}$  – rotor resistance for  $n$ -th MMF harmonic  
 $X_{ln}$  – rotor leakage reactance for  $n$ -th MMF harmonic  
 $X_{mn}$  – magnetization reactance for  $n$ -th MMF harmonic  
 $Z_C$  – capacitive impedance connected in series with auxiliary winding  
 $P$  – poles number  
 $\omega_s, s$  – synchronous speed [rad/sec] and slip  
 $n$  – harmonics order

## II. INTRODUCTION

Single-phase and two-phase induction machines are widely used in commercial applications due to their cost and high reliability. Significant performance deterioration of the systems driven by single or two-phase induction machines may appear due to winding harmonics that create parasitic torques at all speeds, typically causing “dips” in the torque/speed characteristic. Core and rotor copper losses are also increased due to the MMF harmonics effect and thus the motor efficiency is diminished. The study of harmonics effect in single-phase induction motors began about 40 years ago [6-7]. Both odd and even harmonics effect have been considered using the double revolving field theory [1-2]. The other developed methods for the analysis of the single-phase induction motor, i.e. symmetrical components and cross-field

methods, can be adapted for modeling the MMF harmonic effects. This paper presents a unified approach on these methods that demonstrates the equivalence between models and shows how the equivalent circuit elements can be interchanged from one method to another.

The following assumptions are made:

1. The stator windings are built with half-cycle symmetry – a common condition in the mass produced single-phase induction motors – and consequently only the odd MMF harmonics are considered.
2. All the MMF harmonics experience the same level of saturation.
3. The rotor current is treated as a current sheet that varies as a true harmonic function with respect to the position around the air-gap.
4. The effect of skewing is ignored. However, including a skew leakage reactance in the equivalent circuit and reducing the magnetizing reactance accordingly can further consider this effect [14].

Fig. 1 shows a general equivalent circuit of the single-phase induction motor connections. The starting impedance,  $Z_C$  is detailed in its possible components. Experimental torque/speed curves were obtained for three capacitor-run motors, with various main and auxiliary winding distributions. Comparisons between the theoretical and experimental curves show reasonable agreement, with sufficient correlation to provide important guidance on the overall effect of the winding harmonics and the extent to which imperfections in the winding distribution are tolerable. The speed of calculation is important because of the large number of possible cases requiring analysis and interpretation, justifying the development of an analytical method in preference to a finite-element approach that may be more time consuming.

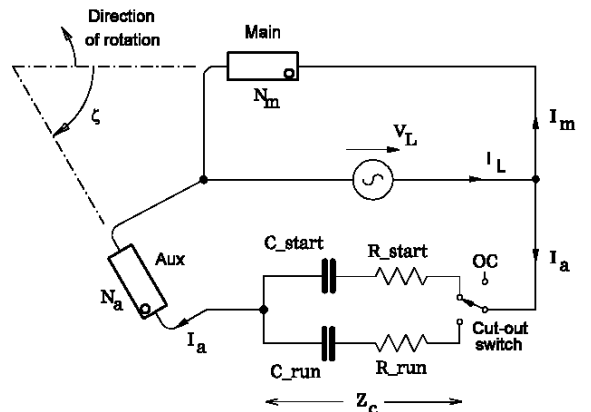


Fig. 1 Equivalent circuit of the single-phase induction motor connections

## III. THEORY

*Forward and backward revolving field method*

The forward- and backward-revolving field method is generally attributed to Morrill [1]. The approach described here is essentially a summary of the lucid account given by Veinott [2], with the addition of the iron loss  $W_{Fe}$  that is represented in the equivalent circuit by  $R_c$ . The variables are expressed as phasors using complex numbers.

Fig. 2 shows the revolving field method applied to a single-phase induction motor when capacitive impedance is in series with the auxiliary winding. Only the fundamental and the 3<sup>rd</sup> MMF harmonic are illustrated. For the analysis of winding harmonics, the permeance variation caused by the slot openings is neglected. The space harmonics are of odd order and rotate at subsynchronous speeds in both the forward and reverse directions. The impedances presented to the positive-sequence (forward) and negative-sequence (backward) harmonic MMF distributions are approximated using the following relations:

$$\mathbf{Z}_{fn} = \frac{0.5}{\frac{1}{jX_{mn}} + \frac{1}{R_m + j \cdot [1+n(1-s)]X_{lm}}} \quad (1)$$

$$\mathbf{Z}_{bn} = \frac{0.5}{\frac{1}{jX_{mn}} + \frac{1}{R_m + j \cdot [1-n(1-s)]X_{lm}}} \quad (2)$$

The magnetization reactance and the rotor leakage reactance for the  $n$ -th harmonic order MMF may be approximated as a function of the reactances corresponding to the fundamental spatial MMF that includes the saturation effect:

$$X_{mn} = \left( \frac{k_{wn}}{k_{w1}} \right)^2 \frac{X_m}{n^2} \quad (3)$$

$$X_{ln} = \left( \frac{k_{wn}}{k_{w1}} \right)^2 X_{lr}$$

The rotor resistance for higher harmonics is the same as for a motor with  $nP$  poles number. So, we can use the approximation:

$$R_m = R_{bar} \left( \frac{k_{wn}}{k_{w1}} \right)^2 + \frac{R_{endring}}{n^2} \quad (4)$$

Note that the bar resistance  $R_{bar}$  and the end-ring resistance  $R_{endring}$  are computed taking into account the skin-effect and the temperature effect [17].

The effective turns ratio that determines the  $n$ -th MMF harmonic interaction (forward and backward fields) is:

$$a_n = \frac{T_{ph\ aux}}{T_{ph\ main}} \cdot \frac{k_{wn\ aux}}{k_{wn}} \quad (5)$$

The harmonic field of order  $n = (4k - 1)$  will determine a rotation in the opposite sense with the fundamental flux wave, while the harmonic field of order  $n = (4k + 1)$  rotates in the same sense with the fundamental. The space MMF harmonics effect is more important at low speed and will diminish the

starting torque. Note that the previously described equivalent circuits employ variable value parameters: magnetising reactances  $X_{mn}$  with the saturation level and rotor resistance with the skin-depth penetration level. The harmonics inductances are determined from the fundamental values using (3-4).

The resultant torque is computed as:

$$T_e = \frac{P}{2} \frac{1}{\omega_s} \left[ (T_f - T_b) + \dots + (T_{fn} - T_{bn}) \right] \quad (6)$$

where the torque produced by the fundamental field is given by:

$$\begin{aligned} T_1 &= \frac{P}{2} \frac{1}{\omega_s} (T_f - T_b) \\ T_f &= \text{Re}(\mathbf{Z}_f) |I_m - jaI_a|^2 \\ T_b &= \text{Re}(\mathbf{Z}_b) |I_m + jaI_a|^2 \end{aligned} \quad (7)$$

The following relations give the torque produced by the  $n$ -th harmonic field:

$$\begin{aligned} T_n &= \frac{P}{2} \frac{1}{\omega_s} (T_{fn} - T_{bn}) \\ T_{fn} &= n \text{Re}(\mathbf{Z}_{fn}) |I_m - ja_n I_a|^2 \\ T_{bn} &= n \text{Re}(\mathbf{Z}_{bn}) |I_m + ja_n I_a|^2 \end{aligned} \quad (8)$$

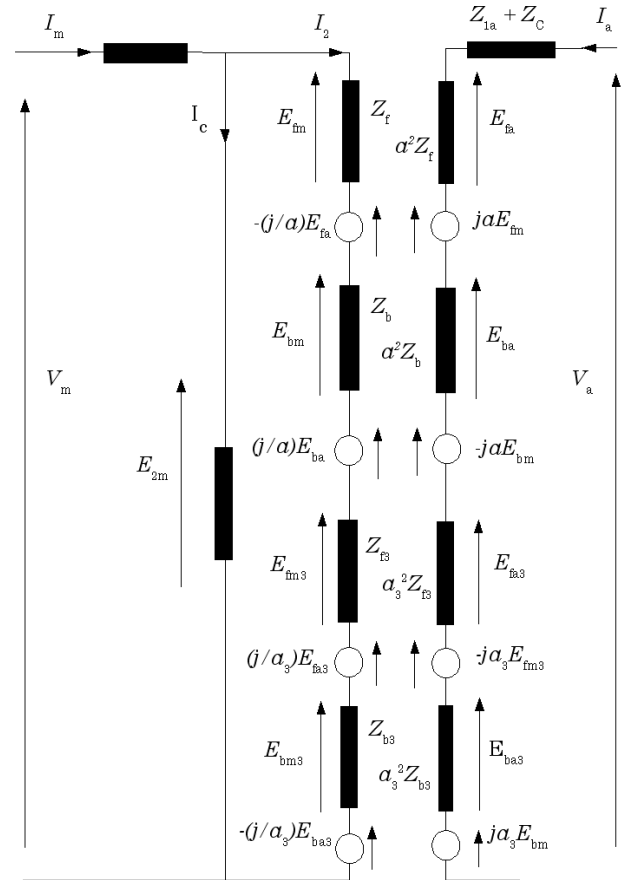


Fig. 2 Equivalent circuit of 1-phase induction motor with capacitor connection using the forward and backward field theory.

$$n = 4k - 1$$

$$T_n = \frac{P}{2} \frac{1}{\omega_s} (T_{fn} - T_{bn})$$

$$T_{fn} = n \operatorname{Re}(\mathbf{Z}_{fn}) |I_m + ja_n I_a|^2$$

$$T_{bn} = n \operatorname{Re}(\mathbf{Z}_{bn}) |I_m - ja_n I_a|^2$$
(9)

Eqs. (8) and (9) show that the main winding distribution is the main source of the harmonic torque, i.e.:

a) a very low winding factor for the  $n$ -th harmonic of the *main winding* eliminates the corresponding harmonic torque regardless of the auxiliary space distribution;

b) a very low winding factor for the  $n$ -th harmonic of the *auxiliary winding* does not eliminate the corresponding harmonic torque if the main winding has a significant  $n$ -th harmonic winding factor.

For higher order harmonics, the torque must be multiplied by the order of the harmonic. The  $n$ -th harmonic field produces a torque similar to a motor with  $n$  times the number of poles of the fundamental field. Usually, the auxiliary winding is displaced 90 electrical degrees from the main winding of the fundamental. This displacement is  $n$  times 90 electrical degrees for the  $n$ -th harmonic.

#### Symmetrical components method

Fig. 3 shows the symmetrical-component model where only the fundamental and the 3<sup>rd</sup> MMF harmonic are illustrated. The model for the fundamental MMF was originally described by Veinott,[2] and Suhr,[3].

By association with the forward-backward field method, the positive sequence corresponds to the forward rotating field and the negative sequence to the backward rotating field.

When the original revolving-field and symmetrical-component theories were first developed, practical computation of the results was a laborious manual process. With fixed values for the iron-loss resistors, the currents can be calculated explicitly, and in this case the computational burden is not greatly increased by including them; but there remains the problem of knowing what values to use.

The approach described here relies on two elements not available to the original authors: one is the extremely fast solution by computer, and the other is the ability to estimate the iron loss independently from the flux-density waveforms (which themselves can now be computed numerically). Indeed it is possible to re-evaluate the iron loss recursively from the flux-density waveforms as the solution proceeds, causing  $R_{cf}$  and  $R_{cb}$  to vary. It is true that the resistors  $R_{cf}$  and  $R_{cb}$  represent the iron loss in the electrical equivalent circuit and improve the calculation of input power and power factor. However, in the split-phase induction motor there are so many other departures from the ideal model, that this enhancement may make little difference to the overall accuracy.

For example, stray loss, inter-bar currents, winding harmonics, and various manufacturing imperfections may have a combined effect that is greater than the iron loss, which is often relatively small in these motors. The values of the resistors  $R_{cf}$  and  $R_{cb}$  cannot be measured directly, but only roughly correlated with a series of calculations over a range of operating conditions.

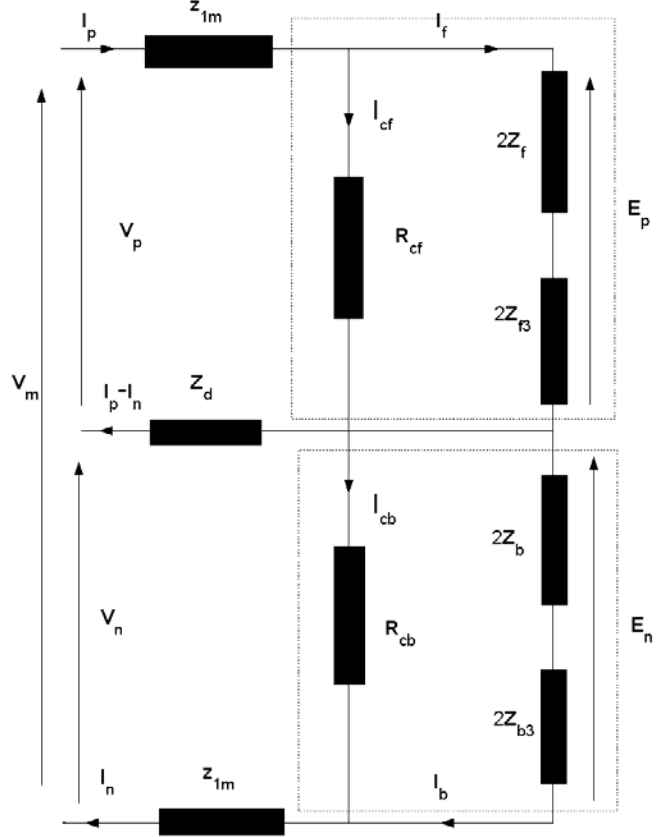


Fig.3 Equivalent circuit of 1-phase induction motor with capacitor connection using the symmetrical components theory.

For this reason it is an advantage to have more than one analytical model, and in the next section a third method is described — the cross-field model — which includes the iron-loss resistors corresponding to the main and auxiliary winding circuits.

The impedances presented to the positive-sequence and negative-sequence harmonic MMF distributions are approximated using the following relations:

$$Z_{in} = \frac{0.5 \alpha_n}{\frac{1}{jX_{mn}} + \frac{1 + n(1-s)}{R_m + j \cdot [1 + n(1-s)] X_{lm}}} \quad (10)$$

$$Z_{in} = \frac{0.5 \alpha_n}{\frac{1}{jX_{mn}} + \frac{1 - n(1-s)}{R_m + j \cdot [1 - n(1-s)] X_{lm}}} \quad (11)$$

The magnetization reactance and the rotor leakage reactance for the  $n$ -th harmonic order MMF may be approximated with similar relations to forward and backward field method (3-4).

The coefficient  $\alpha_n$  is computed as:

$$\alpha_n = 0.5 \left[ 1 + \left( \frac{k_{wn \text{ aux}} k_{w1}}{k_{w1 \text{ aux}} k_{wn}} \right)^2 \right] \quad (12)$$

The coefficient  $\alpha_n$  is introduced to take into account the fact that  $n$ -th MMF harmonic interaction (positive and negative sequence fields) has different effective turns ratio which is  $\alpha_n$  (6). The transformation from the circuit in Fig. 2 (physical

rotating fields) and the circuit from Fig. 3 (fictitious symmetrical components fields) can be done if the forward and backward impedances from the auxiliary winding are expressed using the same effective turns ratio  $a$ . Thus, it would seem necessary to multiply the  $n$ -th harmonic impedances with the ratio  $(a_n/a)^2$ . On the other hand this multiplication would change the harmonic impedance value that is used in the main winding circuit. A possible solution is to use an averaging factor  $\alpha_n$ , which will apply to both forward and backward components of the  $n$ -th space harmonic impedance. A comparison between equivalent circuits in Figs. 2 and 3 shows that if  $a = a_n$  then the rotating forward and backward fields method and symmetrical components method will predict identical results as  $\alpha_n = 1$  for this particular case. If  $k_{wn}$  or  $k_{wnaux}$  are smaller than 0.02, it is practice to set  $\alpha_n = 0$ .

The resultant torque is computed as:

$$T_e = \frac{P}{2} \frac{1}{\omega_s} \left[ (T_f - T_b) \pm \dots \pm (T_{fn} - T_{bn}) \right] \quad (13)$$

where the relations give the torque produced by the  $n$ -th harmonic field:

$$\begin{aligned} T_n &= \frac{P}{2} \frac{1}{\omega_s} (T_{fn} - T_{bn}) \\ T_{fn} &= 2n \operatorname{Re}(\mathbf{Z}_{fn}) |I_f|^2 \\ T_{bn} &= 2n \operatorname{Re}(\mathbf{Z}_{bn}) |I_b|^2 \end{aligned} \quad (14)$$

Note the sign change when including different  $n$ -th harmonics order. The harmonics 3, 7, 11,  $4k - 1$ , determine a reversed rotation sense as compared to the fundamental field, while harmonics 5, 9, 12,  $4k + 1$  determine the same rotation sense with the fundamental field.

### Cross-field method

Fig. 4 shows the cross-field model where only the fundamental and the 3<sup>rd</sup> MMF harmonic are illustrated. The model for the fundamental MMF was originally described by Puchstein and Lloyd [4], and Trickey [5]. It assumes a stationary reference frame fixed to the stator and modern theory describes this method as two-axis or  $dq$  axis models [12, 15, 16]. This method has a better physical correlation with the actual motor. The main and auxiliary winding circuits are uncoupled and modeled individually, interacting with the entire rotor MMF harmonics. Each phase contribution to the torque production may be easily identified.

The magnetization reactance and the rotor leakage reactance for the  $n$ -th harmonic order MMF may be approximated with similar relations to forward and backward field method (3-4). The equivalent iron-loss resistances,  $r_{Cm}$  and  $r_{Ca}$  are modelled as in [18] with the assumption:

$$r_{Ca} = a^2 r_{Cm} \quad (16)$$

The per unit speed term that appears in the induced EMFs for the  $n$ -th MMF harmonic circuit is:

$$S_n = 1 - [1 + n(1-s)] = n(1-s) \quad (17)$$

The resultant torque is computed as:

$$T_e = \frac{P}{2} \frac{1}{\omega_s} (T_1 - T_3 + T_5 - \dots \pm T_n) \quad (18)$$

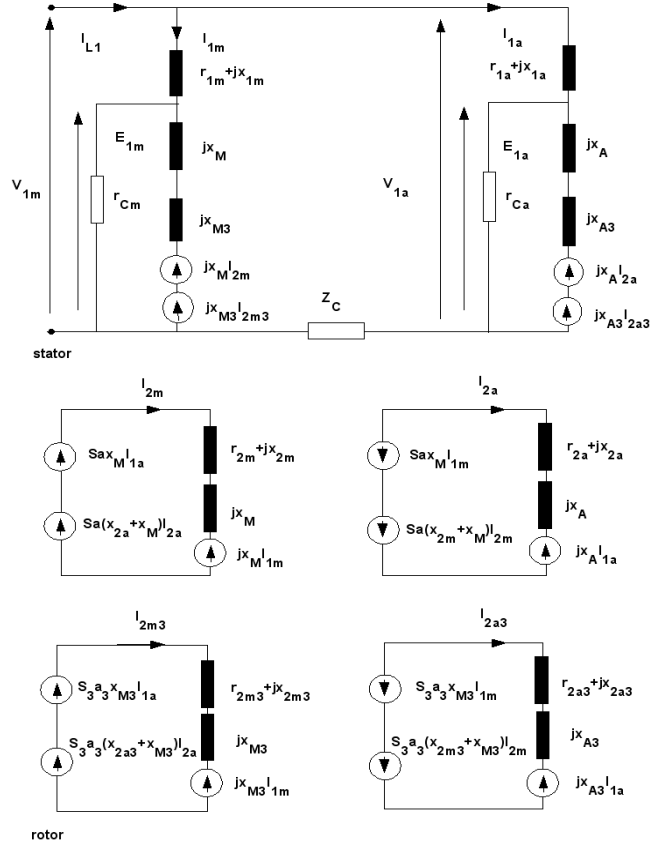


Fig. 4 Equivalent circuit of 1-phase induction motor with capacitor connection using the cross-field theory.

where the torque produced by the fundamental field is:

$$T_1 = a \frac{P X_m}{2 \omega_s} \operatorname{Re} \left[ (I_{1m} - I_{cm})^* \cdot I_{2a} - (I_{1a} - I_{ca})^* \cdot I_{2m} \right] \quad (19)$$

while the torque produced by the  $n$ -th harmonic field is given by:

$$T_n = a_n \frac{P X_{mn}}{2 \omega_s} \operatorname{Re} \left[ (I_{1m} - I_{cm})^* \cdot I_{2an} - (I_{1a} - I_{ca})^* \cdot I_{2mn} \right] \quad (20)$$

where  $a_n$  is computed with (5) and  $I_{cm}$ ,  $I_{ca}$  represent the currents associated with the core loss in the main winding and auxiliary winding respectively.

Note the sign change when including different  $n$ -th harmonics order. The harmonics 3, 7, 11,  $4k - 1$ , determine a reversed rotation sense as compared to the fundamental field, while harmonics 5, 9, 12,  $4k + 1$  determine the same rotation sense with the fundamental field.

The circuit equations representing Fig. 4 may be expressed as a matrix system [15] and thus any harmonic circuit may be easily included. The core-loss variation with the current level is addressed by an initial calculation of the total core losses from an estimate of the flux-density waveforms, extract the values of the corresponding EMFs,  $E_{1m}$ ,  $E_{1a}$  and use a recursive method until  $r_{Cm}$  and  $r_{Ca}$  converge to a steady-state value.

The cross-field and forward-backward field methods will produce identical results if the core losses are neglected. However, as the experiments from the next section showed,

the difference introduced in the computed results between the forward-backward fields and the cross-field methods is not significant.

This result is in line with the idea that various locations of the equivalent core-loss resistance in the equivalent circuit do not change the prediction of the overall motor performance. The symmetrical components method is employing an average of the  $n$ -th harmonic impedance in the stator windings circuit, and thus will predict identical results with the other two methods only for the case when the stator windings have the same distribution or when the MMF harmonics of the main winding may be neglected.

#### IV. COMPARISON WITH EXPERIMENTAL DATA

All the previously described methods are validated on three capacitor-run motors with parameters detailed in Annex.

In Table I the winding factors up to the 7<sup>th</sup> space harmonic are presented, where  $k_{wn\ main}$  and  $k_{wn\ aux}$  stand for main and auxiliary windings harmonics factors. The equivalent circuit elements from Figs. 2-4 are estimated using analytical and numerical methods [19-20].

Figs. 5, 9, 13 show the experimental and computed torque vs speed results when both stator windings are energized, using all three methods for motor 1, motor 2 and motor 3, respectively.

Figs. 6, 10, 14 show the experimental and computed torque vs speed results when only main winding is energized, using all three methods for motor 1, motor 2 and motor 3, respectively.

Figs. 7, 11, 15 show the experimental and computed line current vs speed results using all three methods for motor 1, motor 2 and motor 3, respectively.

Figs. 8, 12, 16 show the experimental and computed efficiency vs speed results using all three methods for motor 1, motor 2 and motor 3, respectively.

One should note for motor 1, that while the forward-backward field and the cross-field methods predict almost similar results in very good agreement with the test data, the symmetrical component method underestimates the torque values between starting and break-down points. The measurements and computations performed for the case when just the main winding is energized (Fig. 6), show that the symmetrical components method overestimates the 3<sup>rd</sup> harmonic effect. Essentially this is due to the averaging factor  $\alpha_n$  from (12). This factor would allow a correct model for the space harmonics effect only if the stator windings have a similar distribution or if the main winding has a low harmonics content. For rated load points, all methods lead to results that give good agreement with test data.

Motor 2 is an example where the main winding has a very low 3<sup>rd</sup> harmonic content while the auxiliary winding contains very high 3<sup>rd</sup>, 5<sup>th</sup> and 7<sup>th</sup> MMF harmonics.

Two main observations are valid for this case:

- a 3<sup>rd</sup> strong harmonic in the auxiliary winding is practically not observable in the torque vs speed curve shape as long as the 3<sup>rd</sup> harmonic from the main winding is very low;
- even if the stator windings do not have an identical distribution, i.e. identical winding factors, the symmetrical component method predicts similar results with the other two

TABLE I

WINDING FACTORS FOR THE TESTED MOTORS

Winding factor	Motor1	Motor2	Motor3
$k_{w1\ main}$	0.8815	0.831	0.9029
$k_{w3\ main}$	0.1944	0.0098	0.3080
$k_{w5\ main}$	0.2540	0.1721	0.1936
$k_{w7\ main}$	0.0442	0.1321	0.1485
$k_{w1\ aux}$	0.9262	0.9577	0.9029
$k_{w3\ aux}$	0.4385	0.6533	0.3080
$k_{w5\ aux}$	0.1021	0.2053	0.1936
$k_{w7\ aux}$	0.2544	0.1576	0.1485

methods if the values for the main and auxiliary winding factors are not significantly different. Practically, a harmonic winding factors ratio ( $k_{wn} / k_{wnaux}$ ) in the range 0.8 ... 1.2 is considered to lead to similar results for all three computation methods. As mentioned in Section III, in connection with the forward-backward field method, a very low winding factor for the  $n$ -th harmonic of the *main winding* eliminates the corresponding harmonic torque regardless of the auxiliary space distribution. This is an important feature that allows the implementation of an auxiliary winding that maximises the starting capabilities and allows a uniform slot fill factor.

All three computation methods lead to similar results in good agreement with test data. Note that the different implementations of the core loss equivalent resistance do not influence significantly the overall results.

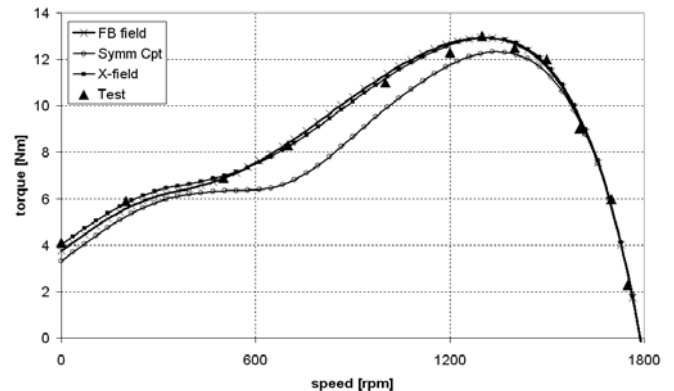


Fig. 5. Experimental and computed torque vs. speed for Motor 1 – energized both stator windings (see Table I).

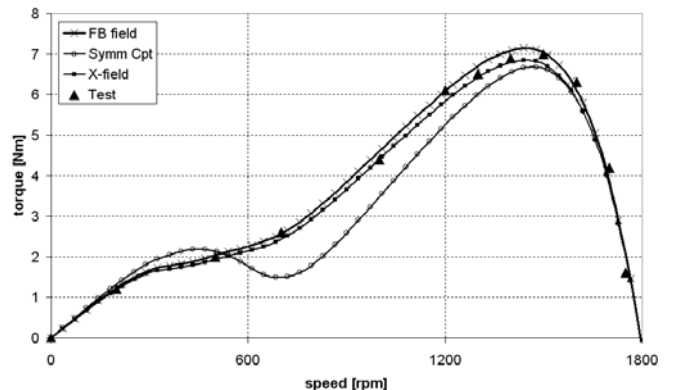


Fig. 6. Experimental and computed torque vs. speed for Motor 1 – energized main winding only (see Table I).

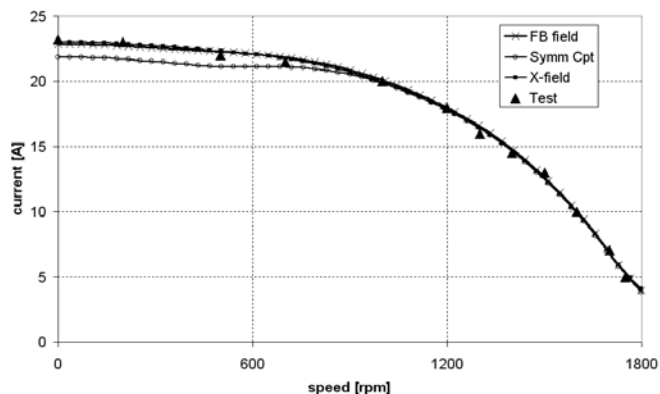


Fig. 7 Experimental and computed current vs. speed for Motor 1 – energized both stator windings (see Table I).

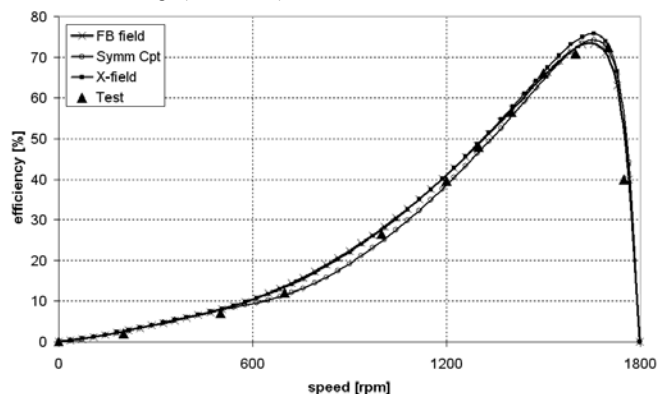


Fig. 8 Experimental and computed efficiency vs. speed for Motor 1 – energized both stator windings (see Table I).

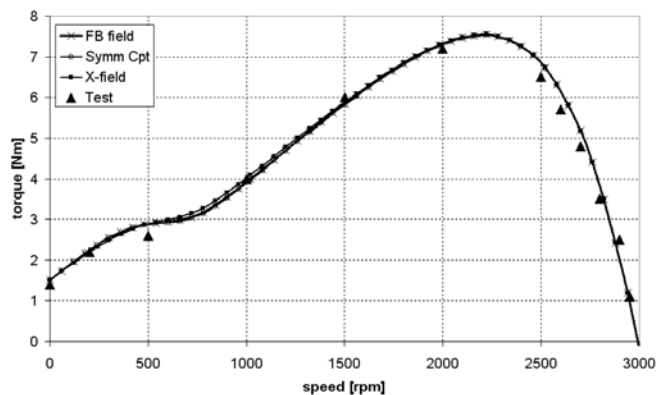


Fig. 9. Experimental and computed torque vs. speed for Motor 2 – energized both stator windings (see Table I).

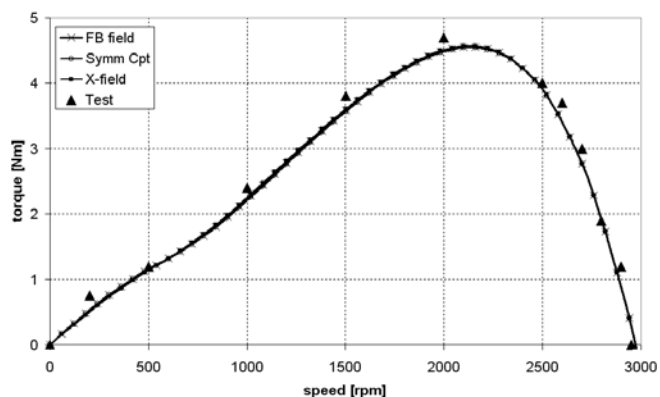


Fig. 10. Experimental and computed torque vs. speed for Motor 2 – energized main winding only (see Table I).

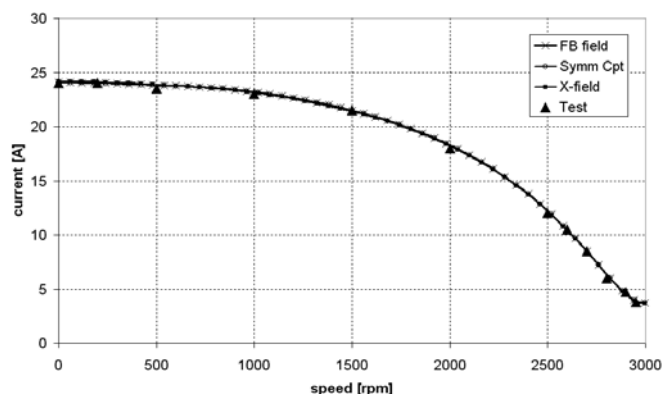


Fig. 11 Experimental and computed current vs. speed for Motor 2 – energized both stator windings (see Table I).

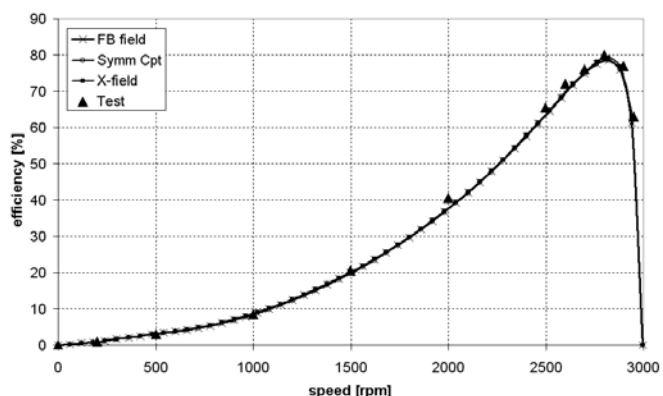


Fig. 12 Experimental and computed efficiency vs. speed for Motor 2 – energized both stator windings (see Table I).

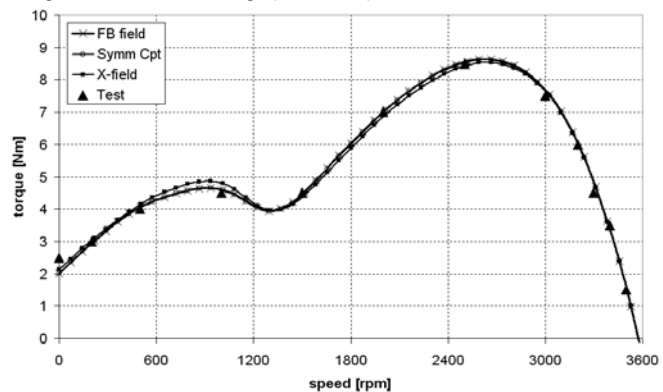


Fig. 13. Experimental and computed torque vs. speed for Motor 3 – energized both stator windings (see Table I).

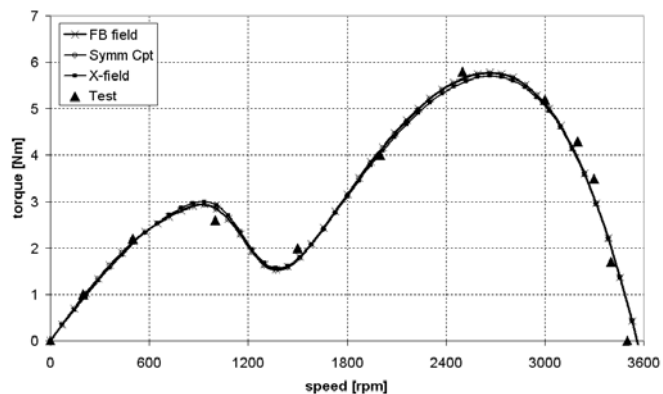


Fig. 14. Experimental and computed torque vs. speed for Motor 3 – energized main winding only (see Table I).

## ANNEX

## MOTORS PARAMETERS

1-phase capacitor-run induction motors:

Motor	# 1	#2	#3
Voltage [V]	220	220	220
Frequency [Hz]	60	50	60
Poles	4	2	2
Capacitor [ $\mu$ F]	40	25	35
Rated power [W]	1100	1000	1875
Rated current [A]	7.1	6.3	11.75
Turn ratio $a$	1.097	0.955	1.48

## REFERENCES

- Morrill, WJ, "The revolving-field theory of the capacitor motor", *Trans AIEE*, April 1929, pp. 614-632.
- Veinott, CG, *Theory and design of small induction motors*, McGraw-Hill, New York, 1959
- Suhr, FW, "Symmetrical components as applied to the single-phase induction motor", *Trans.AIEE*, Vol. 64, September 1945, pp. 651-655
- Puchstein, AF and Lloyd, TC, "The cross-field theory of the capacitor motor", *Trans. AIEE*, Vol. 60, February 1941, pp. 58-63.
- Trickey, PH, "Capacitor motor performance calculations by the cross-field theory", *Trans. AIEE*, Vol.76, February 1957, pp. 1547-1553.
- Buchanan, L.W. "An equivalent circuit for a single-phase motor having space harmonics in its magnetic field" *IEEE Transactions, PAS-84*, November 1965, pp. 999 – 1007
- Davis, J. H. and Novotny, D. W. "Equivalent circuits for single-phase squirrel-cage induction machines with both odd and even order MMF harmonics" *IEEE PAS-88*, July 1969, pp. 1080 – 1086
- Miller, TJE, *SPEED's Electric Motors*, Magna Physics, ISBN 1-881855-10-4
- Heartz, R.P. and Saunders, R.M, "Harmonics due to slots in electric machines" *AIEE Trans. (Power Apparatus System)* August 1954, Vol. 73, pp. 946-949
- Fudeh H. R., and Ong, C. M., "Modeling and analysis of induction machines containing space harmonics" Part I, II, III, *IEEE PAS-102*, August 1983, pp. 2608 – 2628
- Boldea, I., Dumitrescu, T., Nasar, S. "Unified analysis of 1-phase AC motors having capacitors in auxiliary windings" *Energy Conversion IEEE Transactions on*, Vol. 14, No.3, September 1999, pp. 577-58
- Krause, PC, Wasynczuk, O and Sudhoff, SD: *Analysis of electric machinery*, IEEE Press, NJ, 1995
- Alger PL *Induction machines, their behavior and uses*, Gordon & Breach Science Publishers, New York, London, Paris, Second Edition, 1970
- Williamson, S., Smith, AC: "A unified approach to the analysis of single-phase induction motor", *IEEE Trans. on Ind. Appl.*, Vol. 35, No. 4, July-August 1999, pp. 837-843
- Dorrell, D.G. "Analysis of split-phase induction motors using an impedance matrix" *Conf Rec. PEMD 2004*, Edinburgh, March 2004, Vol. 2, pp. 811-816
- Popescu, M. Inel, D.M, Dorrell D.G.: "Vector control of unsymmetrical two-phase induction motors" *Conf. Rec. IEEE IEMDC 2001*, Boston, MA, May 2001, Vol. 1, pp. 95 – 101.
- Boldea, I and Nassar S.A.: *The induction machine handbook*, CRC Press, 2001
- Rasmussen, CB and Miller, TJE; "Revolving-field polygon technique for performance prediction of single-phase induction motors" *IEEE Trans. on Ind. Appl.* Vol. 39, No 5, Sept.-Oct. 2003, pp:1300 – 1306
- Miller, TJE, McGilp MI, Olaru M. "PC-FEA 5.5 for Windows – Software", SPEED Laboratory, University of Glasgow, Glasgow (UK), 2006
- Miller, TJE and McGilp MI, "PC-IMD 3.5 for Windows – Software", SPEED Laboratory, University of Glasgow, Glasgow (UK), 2006

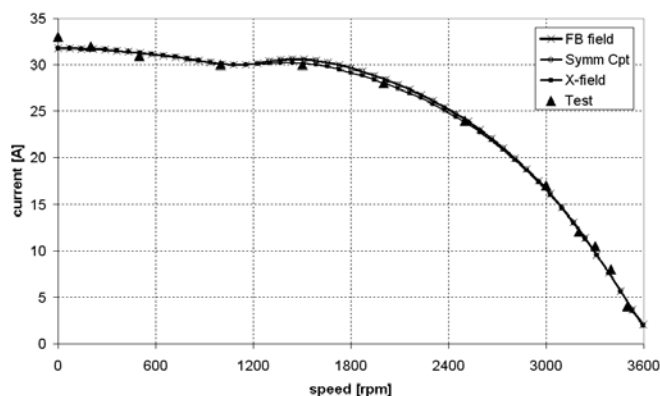


Fig. 15. Experimental and computed current vs. speed for Motor 3 – energized both stator windings (see Table I).

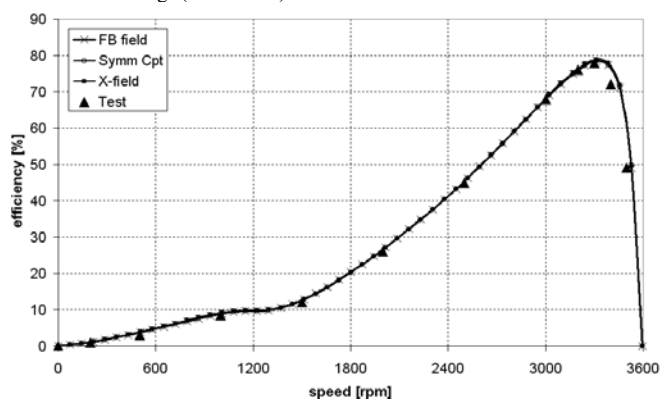


Fig. 16. Experimental and computed efficiency vs. speed for Motor 3 – energized both stator windings (see Table I).

Motor 3 is an example where the main and auxiliary windings have an identical space distribution. For such cases, virtually any computation method may be selected for a good correlation with the test data. The differences between test data and computation that still occur can be explained by the uncertainties in the materials (steel, rotor cage alloy) properties.

## V. CONCLUSIONS

The effects of MMF harmonics can be analytically modeled in single-phase induction motors using any of the three classical methods. The equivalence of the methods is demonstrated in this paper. The forward-backward field and cross field methods may be used for any stator winding distribution and configuration, while the symmetrical components method should be avoided for the cases when both windings have an important but different space harmonics content. The core-loss modelling by the placement of equivalent resistances in various locations within the equivalent circuits has a minor effect on the accurate prediction of the overall motor performance.

## ACKNOWLEDGEMENT

The authors thank their colleagues at Grundfos A/S, Bjerringbro, Denmark; and the SPEED Consortium.